

Article

The Influence of Recipe-Technological Factors on the Resistance to Chloride Attack of Variotropic and Conventional Concrete

Evgenii M. Shcherban¹ , Sergey A. Stel'makh² , Alexey N. Beskopylny^{3,*} , Levon R. Mailyan², Besarion Meskhi⁴ , Valery Varavka⁵, Andrei Chernil'nik² , Diana Elshaeva² and Oxana Ananova⁶

¹ Department of Engineering Geology, Bases, and Foundations, Don State Technical University, 344003 Rostov-on-Don, Russia; au-geen@mail.ru

² Department of Unique Buildings and Constructions Engineering, Don State Technical University, 344003 Rostov-on-Don, Russia; sergej.stelmax@mail.ru (S.A.S.); lrm@aaanet.ru (L.R.M.); chernila_a@mail.ru (A.C.); diana.elshaeva@yandex.ru (D.E.)

³ Department of Transport Systems, Faculty of Roads and Transport Systems, Don State Technical University, 344003 Rostov-on-Don, Russia

⁴ Department of Life Safety and Environmental Protection, Faculty of Life Safety and Environmental Engineering, Don State Technical University, 344003 Rostov-on-Don, Russia; spu-02@donstu.ru

⁵ Research and Education Center "Materials", Don State Technical University, 344003 Rostov-on-Don, Russia; varavkavn@gmail.com

⁶ Department of Marketing and Engineering Economics, Faculty of Innovative Business and Management, Don State Technical University, 344003 Rostov-on-Don, Russia; o_ananova@mail.ru

* Correspondence: besk-an@yandex.ru; Tel.: +7-8632738454



Citation: Shcherban', E.M.; Stel'makh, S.A.; Beskopylny, A.N.; Mailyan, L.R.; Meskhi, B.; Varavka, V.; Chernil'nik, A.; Elshaeva, D.; Ananova, O. The Influence of Recipe-Technological Factors on the Resistance to Chloride Attack of Variotropic and Conventional Concrete. *Infrastructures* **2023**, *8*, 108. <https://doi.org/10.3390/infrastructures8070108>

Academic Editors: Patricia Kara De Maeijer and Davide Lo Presti

Received: 8 May 2023

Revised: 24 May 2023

Accepted: 23 June 2023

Published: 27 June 2023



Copyright: © 2023 by the authors. Licensee MDPI, Basel, Switzerland. This article is an open access article distributed under the terms and conditions of the Creative Commons Attribution (CC BY) license (<https://creativecommons.org/licenses/by/4.0/>).

1. Introduction

The relevance of this study is ensured by the fact that, at present, in the construction industry, there is a need for sustainable building technologies that allow the erection of buildings and structures in complicated engineering, geological, and urban conditions. In areas with floodplain geology, there is also a need for a large number of reservoirs and, as a result, for well-developed transport infrastructure such as bridges and flyovers as well [1–3]. There is a lack of complex, scientifically based technological, material science, and design solutions for universal types of building materials, products, and structures in infrastructural development, especially with regard to structures operated in water bodies.

Given that the issue of durability is directly related to the aggressiveness of environmental conditions, including water, the most important aspect of structural materials will be their resistance to various aggressive influences [4–6].

An increase in the resistance of concrete to corrosion from chloride salts can be achieved through various formulation solutions, which include the introduction of various additives into the concrete mixture. For example, a number of studies have considered the possibility of using rubber waste as an additive that improves the corrosion resistance of concrete. In [7], recycled rubber was introduced instead of a part of fine aggregate in the amount of 5%, 10%, and 15% of its mass, and according to the results of experimental studies, it was found that the most effective increase in the resistance of concrete to chloride erosion can be achieved with a rubber content in the amount of 10%. Recycled rubber in [8] was also introduced to replace some of the fine aggregates. It has been established that the mechanical properties of concrete during the period of aggressive action improve with an increase in the size of rubber particles and decrease with an increase in the percentage of their content. The best corrosion resistance was recorded for concretes containing rubber particles in the amount of 5%. And conversely, in [9], when rubber crumb was added as a partial replacement for fine filler in the manufacture of columns, a negative effect was observed, expressed as a decrease in the mechanical characteristics and durability of the columns. Additionally, various types of nano additives were studied with the aim of increasing the resistance of concrete to chloride corrosion. For example, in [10], graphene nanoplatelets were used as a nano additive. As a result, it was found that when 0.05% of this additive was introduced into concrete, its strength increased to 20.97%, and its resistance to chlorides increased as well.

In [11], the durability of cement slurries with the addition of TiO_2 was studied. The introduction of carbon nanotubes has been found to reduce the porosity of cement composites, thereby increasing the resistance to chloride penetration, which in turn, has been confirmed by studies [12]. And in [13], an assessment was made of the corrosion resistance of cement mortars modified with the addition of nanosilica. The introduction of 2% nanosilica made it possible to reduce the diffusion coefficient of chloride ions. In [14], nano-attapulgite clay was considered a modifying additive. The introduction of this additive makes it possible to increase the compressive strength of concrete by more than 7%, as well as to reduce the diffusion rate of chlorine ions. Some authors have examined the possibility of using different types of fibers to improve the corrosion resistance of concrete. The use of polypropylene fibers in [15] was found to increase the density of concrete by reducing microporosity, which, in turn, reduced the diffusion rate of chloride ions. In [16], the effect of two types of fiber on the diffusion coefficient of chlorides was evaluated. According to the results of the experiments, it was found that the use of polypropylene fibers led to a decrease in the diffusion coefficient of chlorides, which coincides with the results of [15], while the addition of steel fibers had the opposite effect. The joint introduction of polypropylene and basalt fibers into concrete helps to reduce the diffusion of chlorides, which was confirmed by the results of [17]. Interestingly, in a study [18] where marble and granite dust were introduced instead of part of the cement, it was found to increase the corrosion resistance of concrete. According to the results of the research, mixtures with 20% content of marble and granite dust showed a higher potential for corrosion. Other studies have also investigated the effects of slag and metakaolin [19] on the durability of concrete, and slag has been used both as an additive to concrete [19] and as a component of cement [20]. It should be noted that there is a large number of works devoted to the prediction of the durability of reinforced concrete structures operated in aggressive chloride environments, as well as to the study of the mechanism of destruction of these structures under conditions of chloride attack. Examples of such studies are found in [21–24]. The complex effects of various nano additives and fibers on the durability of concretes and mortars, including marine structures, were already considered earlier in [25–28]. Reinforced concrete structural components of offshore structures are exposed to corrosion due to the impact of salts and require an analysis of durability indicators to obtain more accurate predictions of the occurrence of

corrosion and its course [29]. At the same time, when studying the durability of reinforced concrete, it is important to take into account the effect of chlorides on the corrosion of steel and welds [30,31], taking into account the properties of concrete [31]. There are quite a few studies devoted to the numerical simulation of the transport and diffusion of chlorides in concrete and reinforced concrete elements under cyclic exposure [32,33]. Works on the creation of multifactorial models of the penetration of chlorides into reinforced concrete structures under various conditions are also widespread [34,35]. In addition to changing the physical and mechanical properties for assessing the destruction of concrete and reinforced concrete caused by chlorides, a common characteristic is an electrical resistivity [36]. To slow down the corrosion of reinforced concrete, various inhibitors are used, the properties of which have been studied by various researchers [37]. The effect of concrete manufacturing technology involving a 3D printer on the course of corrosion and carbonization caused by chlorides is relevant to this study. Concrete printed with a 3D printer is inferior to reference-cast concrete from the same concrete mix in terms of durability [38].

Our review revealed a lack of knowledge about the complex effect of technological and prescriptive factors on the durability of concrete under cyclic chloride attack. Thus, our study will examine the differences in the durability of concretes of various compositions used in structures operated in especially dangerous and high-risk conditions, i.e., to compare and evaluate the differences in the durability of conventional and variotropic concretes made using three different technologies: vibrating, centrifuging and vibro-centrifuging, and modified with the addition of microsilica, under conditions of cyclic chloride attack.

2. Materials and Methods

2.1. Materials

Portland cement of the CEM I 52.5 N brand (Starotsementny plant, Sukhoi Log, Russia) was used as a binder. As a coarse aggregate, crushed stone from the sandstone of a fraction of 5–20 mm from the Obukhov pit (Fedorovsky crushed stone plant, Shakhty, Russia) was used, and quartz sand was used as a fine aggregate (Astakhovsky quarry, Kvarts LLC, Shakhty, Russia). The characteristics of raw materials are presented in Table 1.

Table 1. Characteristics of the raw components of the concrete mix.

Component	Indicator	Actual Value
Portland cement CEM I 52.5 N	Specific surface area (m^2/kg)	340
	Normal consistency of cement paste (%)	27
	Grinding fineness (residue on sieve No. 008) (%)	3.2
	Setting time (min)	
	- start	170
	- end	240
	Bending strength (MPa)	8.1 (28 days)
	Compressive strength (MPa)	54.3 (28 days)
	Tricalcium silicate (%)	67
	Dicalcium silicate (%)	15
	Tricalcium aluminate (%)	8
	Tetracalcium aluminoferrite (%)	10

Table 1. Cont.

Component	Indicator	Actual Value
Crushed sandstone	Crushability (%)	11.8
	The content of lamellar and needle-shaped grains (%)	9.4
	The content of dust and clay particles (%)	0.2
	Content of weak grains (%)	2.2
Quartz sand	Bulk density (kg/m^3)	1428
	Fineness modulus M_f	1.9
	The content of dust and clay particles (%)	1.3
	Clay content in lumps (%)	0.08
	Bulk density (kg/m^3)	1503

As a modifying additive, ultrafine silicon dioxide in the amorphous state was used—microsilica grade MK-85 (Novolipetsk Metallurgical Plant, Lipetsk, Russia) according to the specifications [39], which take into account the main regulatory of the following standards: BS EN 13263-1:2005 + A1:2009 “Silica fume for concrete—Part 1: Definitions, requirements and conformity criteria”; BS EN 934-2:2009 + A1:2012 “Admixtures for concrete, mortar, and grout—Part 2: Concrete admixtures—Definitions, requirements, conformity, marking and labeling”; ASTM C 1240-15 “Standard specification for silica fume used in cementitious mixtures”. Most of the microsilica particles were in the size range from 8 to 30 μm . The chemical composition of microsilica is presented in Table 2.

Table 2. Chemical composition of microsilica MK-85.

Element	SiO_2	Al_2O_3	Fe_2O_3	CaO	MgO	Na_2O	K_2O	C	S
Content (%)	93	0.64	0.69	1.58	1.01	0.61	1.23	0.98	0.26

A 5% solution of sodium chloride NaCl (Mikhailovsky Plant of Chemical Reagents, Barnaul, Russia) was used to simulate the chloride attack.

Polyplast Ligno (Poliplast, Moscow, Russia), an additive based on modified lignosulfonates in the form of a brown aqueous solution with a water mass proportion of not more than 54% and a pH value of at least 4, was used as a plasticizing additive.

2.2. Methods

In order to obtain particles of a given size, silica fume grade MK-85 (Novolipetsk Iron and Steel Works, Lipetsk, Russia) was subjected to additional mechanical processing by grinding in an Activator-4M planetary ball mill (Chemical Machine-Building Plant, Novosibirsk, Russia) for 6 h at 700 rpm, and granulometric analysis was performed on a Microsizer 201C laser particle analyzer (VA Insult, St. Petersburg, Russia).

The technological stages of manufacturing vibrated (V), centrifuged (C), and vibro-centrifuged (VC) concrete are presented in Figure 1.

The composition of vibrated concrete was selected according to [40], and the composition of centrifuged and vibro-centrifuged concrete according to [41].

The preparation of the concrete mixture for all types of concrete was carried out according to the methodology, which included the following processes: dosing of the components of the concrete mixture; loading cement and sand into a laboratory concrete mixer BL-10 (ZZBO, Zlatoust, Russia) and mixing them for 60 s; loading coarse aggregate and mixing for 60 s; adding water and stirring the mixture until a homogeneous consistency. The density of the concrete mixture was determined according to [42], and the test for mobility was carried out according to [43]. The vibrated concrete samples were formed

by pouring the concrete mixture into FK-50 metal molds (Komplekt Laboratory, Moscow, Russia) and compacting them on the SMZh-539-220A vibrating platform (IMASH, Armavir, Russia). The centrifugation modes were as follows: distribution of the concrete mixture over the assembled metal form of the annular section for 70 s at a rotation speed of 150 rpm; compaction of the concrete mix in 220 s at 700 rpm. Centrifuge (DSTU, Rostov-on-Don, Russia), according to [44], was used for centrifugal compaction of annular samples. A stone-cutting machine (Helmut, Moscow, Russia) was used to cut the concrete elements of the annular section. The centrifugation modes are described in more detail in previous works [45,46], and the scheme and process of sawing samples of an annular section are shown in Figure 2.

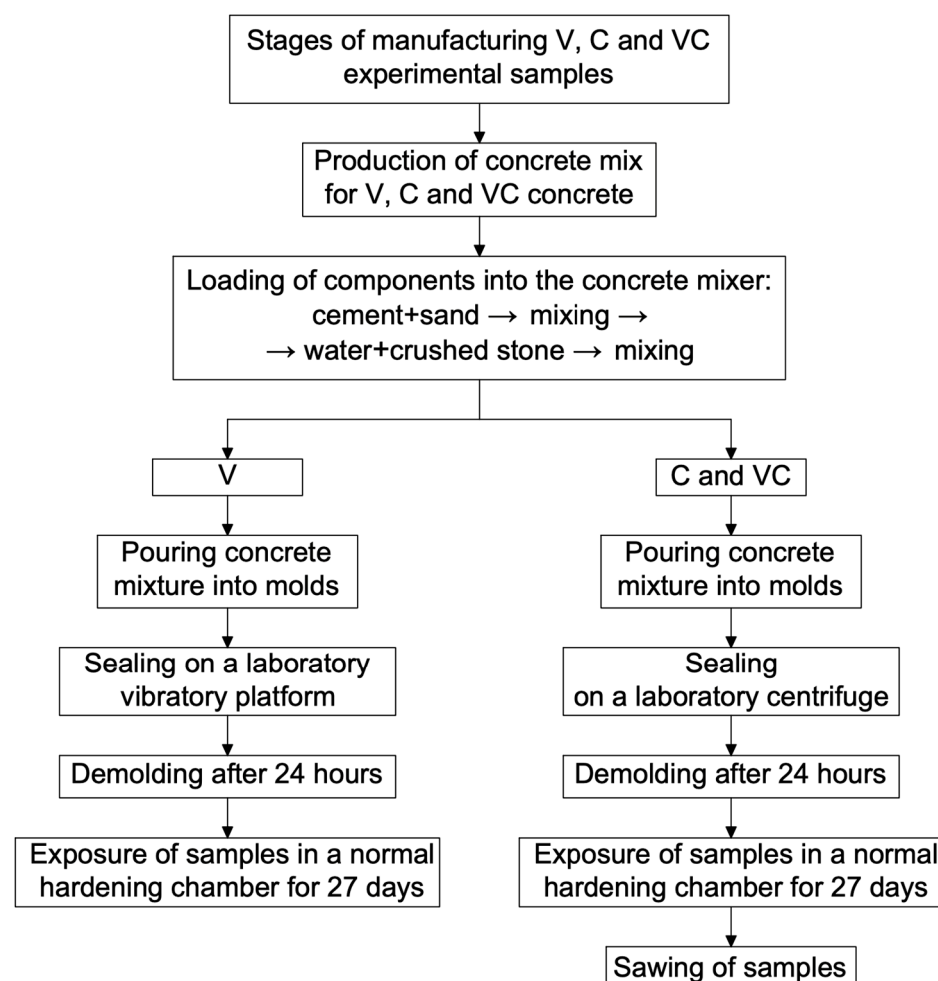


Figure 1. Technological stages of sample production.

In total, according to the results of experimental studies, 150 sample cubes with a size of $70 \times 70 \times 70$ mm for vibrated concrete were made. A similar number of samples were cut from prefabricated centrifuged and vibro-centrifuged concrete elements. In total, 450 concrete cube samples were made and cut.

For the manufacture of concrete using the technology of vibrating, centrifuging, and vibro-centrifuging, concrete mixtures with a certain recipe were used (Table 3). The dosage of the additive was carried out according to the mass of the binder (from the mass of cement and microsilica); that is, part of the binder was replaced by a modifying additive—microsilica of the same mass.

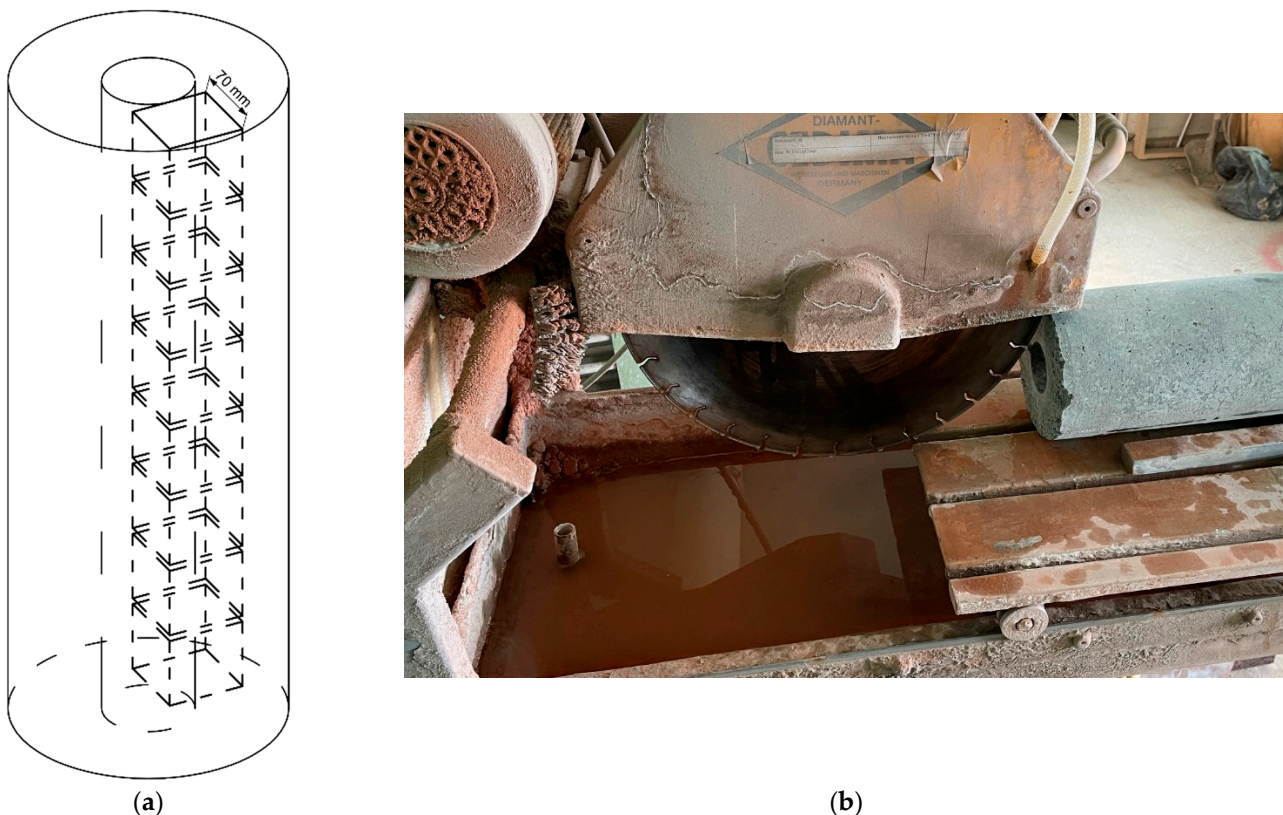


Figure 2. Scheme (a) and photograph of the process (b) of sawing samples of centrifuged and vibro-centrifuged concretes.

Table 3. Recipe of concrete mixtures.

Mixture Type	Cement (kg/m ³)	Water (kg/m ³)	Sand (kg/m ³)	Crushed Stone (kg/m ³)	Microsilica (kg/m ³)	Plasticizer (% by Weight of Binder)
Control V	395	210	792	1045	-	0
V-2	387	210	792	1045	7.9	0.2
V-4	379	210	792	1045	15.8	0.4
V-6	371	210	792	1045	23.7	0.6
V-8	363	210	792	1045	31.6	0.8
Control C/VC	477	205	537	1155	-	0
C/VC-2	468	205	537	1155	9.4	0.2
C/VC-4	458	205	537	1155	19.1	0.4
C/VC-6	448	205	537	1155	28.6	0.6
C/VC-8	439	205	537	1155	38.2	0.8

The characteristics of fresh concrete are presented in Table 4.

Table 4. Characteristics of fresh concrete.

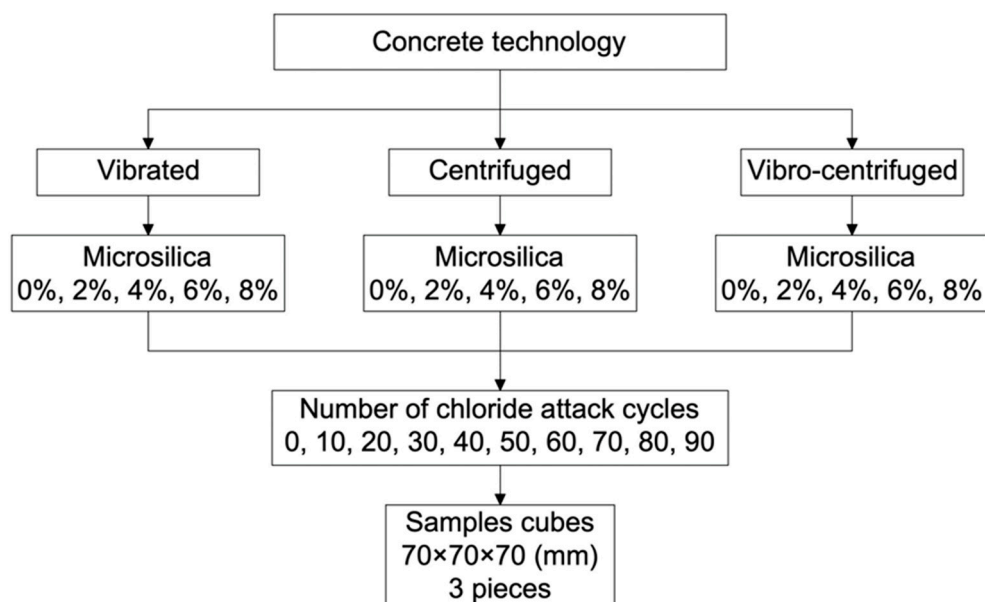
Mixture Type	Density (kg/m ³)	Slump Workability (cm)
Control V	2448	1.5
V-2	2443	1.7
V-4	2440	2.0
V-6	2436	2.1
V-8	2430	2.6
Control C/VC	2378	1.6
C/VC-2	2375	1.8
C/VC-4	2370	2.1
C/VC-6	2368	2.2
C/VC-8	2363	2.4

Solutions for simulating aggressive cyclic chloride attacks were prepared by dissolving NaCl in water.

Changes in the compressive strength of concretes produced by various technologies, subjected to the aggressive action of chloride salts, were studied at the following stages:

- One cycle of moistening–drying of concrete samples consisted of keeping in 5% NaCl solution for 24 h, subsequent extraction from the solution, and drying in a ShS-80-01 SPU oven (Smolensk SKTB SPU, Smolensk, Russia) for 24 h at temperature 50 °C; to maintain the purity of the experiment and the concentration of chloride ions, the solution was changed every 10 days;

- For compressive strength tests, nine control points were established (number of cycles); the plan of experimental studies is shown in Figure 3; compressive strength was determined after every 10 cycles of chloride attack, and the total duration of the experiment was 90 days.

**Figure 3.** Plan of experimental studies.

The process of saturation and drying of samples is shown in Figure 4.



Figure 4. The process of saturation (a) and drying (b) of experimental samples.

The compressive strength of experimental samples was determined in accordance with the requirements [47] on an IP-1000 press (NPK TEHMASH, Neftekamsk, Russia). This procedure complies with the basic regulations for the manufacture and testing of concrete specimens given in the following European Regional Standards:

- EN 12390-1:2009 “Testing hardened concrete—Part 1: Shape, dimensions and other requirements of specimens and molds”;
- EN 12390-2:2009 “Testing hardened concrete—Part 2: Making and curing specimens for strength tests”;
- EN 12390-3:2009 “Testing hardened concrete—Part 3: Compressive strength of test specimens”;
- EN 12390-4:2009 “Testing hardened concrete—Part 4: Compressive strength—Specification for testing machines”.

Photos of testing samples of ordinary vibrated and variotropic concrete are shown in Figure 5.

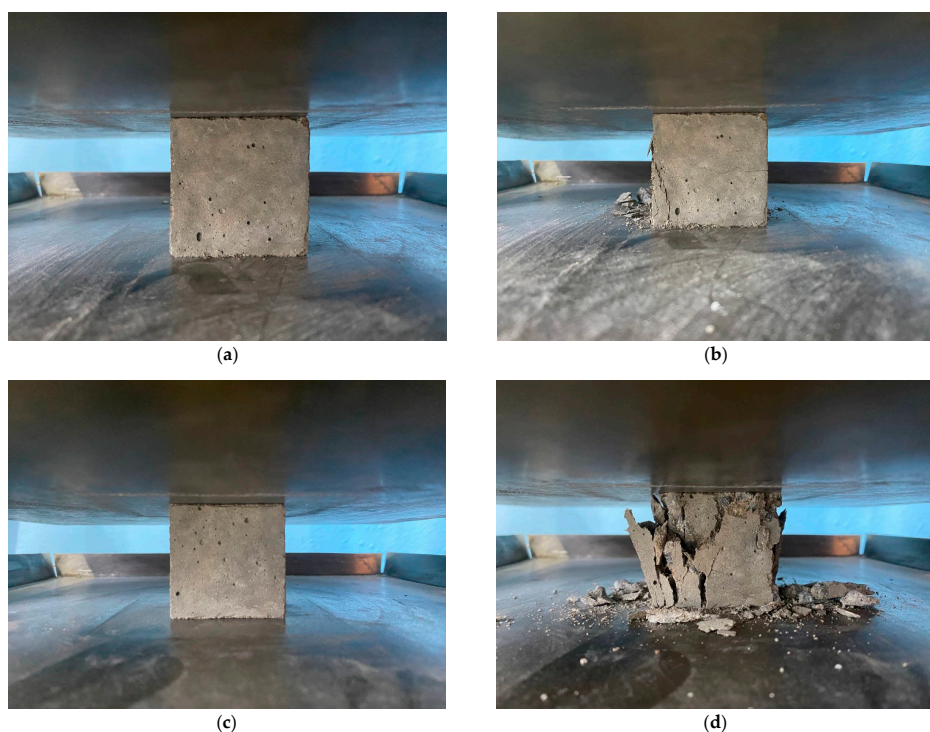


Figure 5. Photographs of tests of samples of variotropic (a,b) and ordinary vibrated (c,d) concrete for compressive strength before failure (a,c) and after failure (b,d).

The verification procedure consisted, firstly, in the use of the basics tested and approved by standard technical documents, and secondly, in the use of materials with known characteristics obtained from manufacturers and confirmed by our own tests. The third aspect of the verification procedure was retesting in order to obtain a representative sample and, thus, the possibility of eliminating erroneous random results. During this work, the accuracy of the dosage of the components of concrete mixtures, the technological parameters for the manufacture of vibrated, centrifuged, and vibro-centrifuged concrete, the conditions and duration of the sulfate attack, and the environmental conditions in which the manufacture and testing were carried out, were observed and remained within acceptable limits.

3. Results and Discussion

3.1. Particle Distribution Curves of the Modifying Additive

The distribution curves of microsilica particles before and after machining are shown in Figure 6.

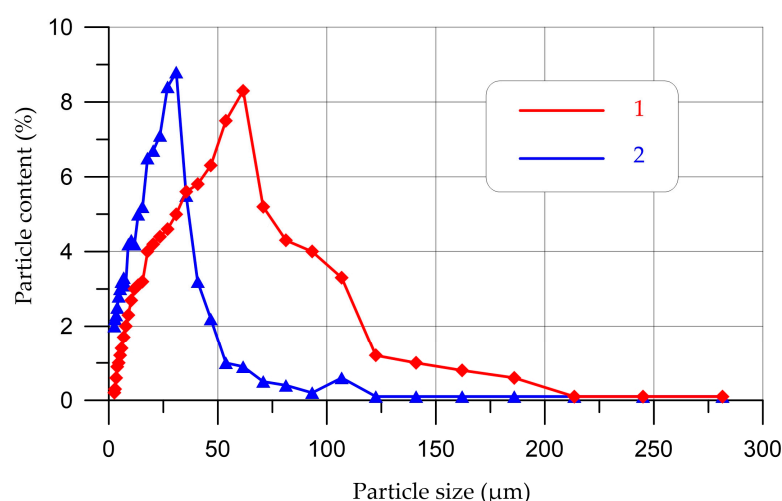


Figure 6. Distribution curves of microsilica particles before mechanical treatment (1) and after (2).

As can be seen from Figure 6, the distribution of microsilica particles before grinding can be characterized as follows. Particles with a size of 2 to 8 μm accounted for 9.3%, from 8 to 30 μm , 36.5%, and from 30 to 285 μm , 54.2%. As for microsilica subjected to mechanical processing, the particle sizes from 2 μm to 8 μm were already 24.4%, from 8 to 30 μm , 60.4%, and for the size range from 30 μm to 285 μm , the total content of microsilica particles was 15.2%.

3.2. Evaluation of the Loss of Compressive Strength of Various Types of Concrete as a Result of Cyclic Chloride Attack

The results of the loss of compressive strength of concretes made using three different technologies, depending on the number of cycles of chloride attack and the percentage of the modifying additive, are shown in Figures 7–11. Figure 7 shows the dependence of the change in compressive strength of concrete samples without additives on the number of cycles of a chloride attack.

Dependences of the strength presented in Figure 7 at 0% microsilica on the number of cycles of chloride attack are well described by Equations (1)–(3) by polynomials of the second degree (R^2 is coefficient of determination)

$$R_{b,cub}^V = 38.50 - 0.0358 x - 0.0005568 x^2, \quad R^2 = 0.978 \quad (1)$$

$$R_{b,cub}^C = 40.51 - 0.00475 x - 0.00060984 x^2, \quad R^2 = 0.981 \quad (2)$$

$$R_{b,cub}^{VC} = 42.14 - 6.06 \times 10^{-5} x - 0.000606 x^2, \quad R^2 = 0.97 \quad (3)$$

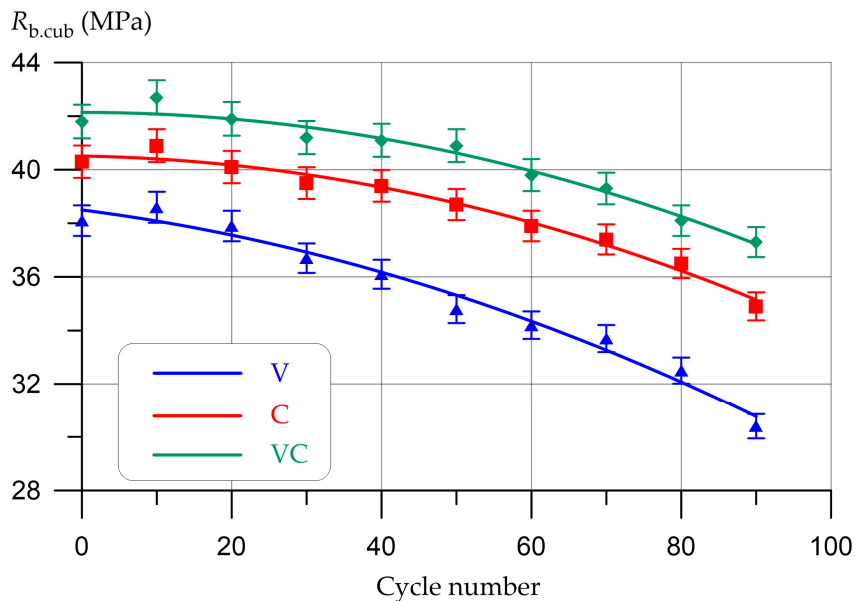


Figure 7. Change in compressive strength of samples V, C, and VC of concrete without modifying additive depending on the number of cycles of chloride attack.

Based on Figure 7, the trend of change in compressive strength can be conditionally divided into three characteristic areas. The loss of compressive strength of vibrated, centrifuged, and vibro-centrifuged concretes after the first 30 cycles of aggressive chloride action of the “wet-dry” type are not so significant in percentage terms compared to the samples of the control composition: for V concrete—3.7%, for C—2.0%, and 1.4% for VC. After 30 to 60 cycles, the strength curves are already steeper downward, and the strength loss for V concrete is 10.2%, for C concrete, 6.0%, and 4.8% for VC concrete. After 60 cycles and up to 90 cycles, the compressive strength decreases even more intensively, and the maximum value of loss of strength for V concrete is 20.2%, for C concrete—13.4%, and 10.8% for VC concrete. The loss of compressive strength with an increase in the number of chloride attack cycles is explained by the fact that calcium chloride compounds are formed as a result of the reaction of chlorides with cement stone. And the presence of chemical influences repeated in time leads to the disintegration of the cement stone or failure in the structure of the composite due to high volumetric pressure because of the formation of large-volume compounds in the pore spaces of concrete. It should be noted that under the alternating effect of moistening and drying, the penetration of chlorides into the concrete is more intense. In the process of wetting, dry concrete absorbs a salty environment; then, in the process of drying, water evaporates from the mouths of the pores, and the salts remain in the concrete. So, as a result of alternating wetting and drying of concrete, there is a diffuse transfer of salts into the depths of the concrete body [4,15,28,48]. According to the results of testing concretes of the control composition, it was found that centrifuged and vibro-centrifuged concretes have a higher resistance to cyclic chloride attack compared to vibrated concrete. This dissimilarity can be primarily explained by the difference between the macrostructures of vibrated concrete and variotropic concretes made using the technology of centrifugal compaction [5,45,46,49]. The denser structure of the outer layer of centrifuged and vibro-centrifuged concretes with closed microporosity better resists a chloride attack.

Figure 8 shows the dependence of the change in compressive strength of concrete samples with an additive in the amount of 2% by weight of the binder on the number of cycles of chloride attack.

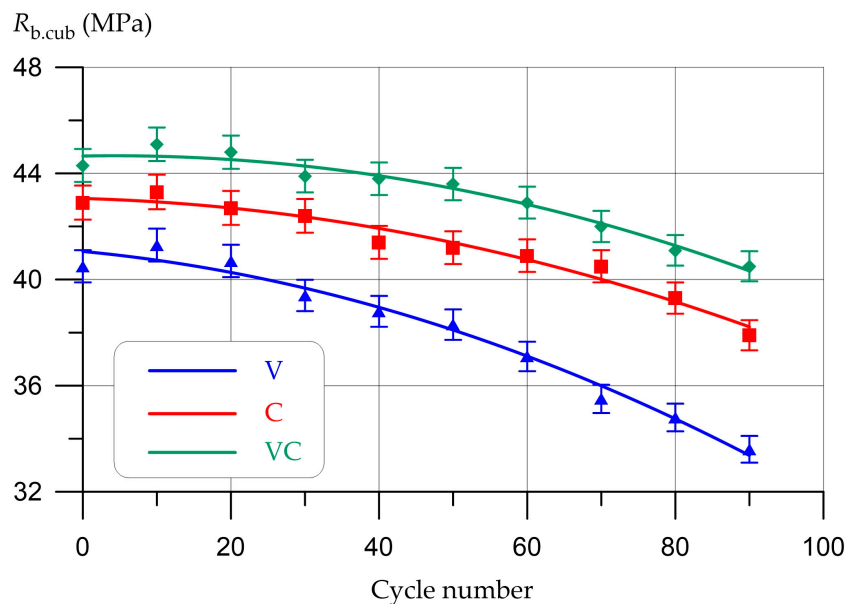


Figure 8. Change in compressive strength of samples V, C, and VC of concrete with 2% silica fume depending on the number of cycles of chloride attack.

Dependences of the strength presented in Figure 8 at 2% microsilica on the number of cycles of a chloride attack are well-described by Equations (4)–(6) by polynomials of the second degree.

$$R_{b.cub}^V = 41.06 - 0.03265 x - 0.0006553 x^2, \quad R^2 = 0.980 \quad (4)$$

$$R_{b.cub}^C = 43.055 - 0.00773 x - 0.0005113 x^2, \quad R^2 = 0.967 \quad (5)$$

$$R_{b.cub}^{VC} = 44.65 + 0.00506 x - 0.0005909 x^2, \quad R^2 = 0.968 \quad (6)$$

As can be seen from Figure 8, the curves of changes in compressive strength V, C, and VC of concretes modified with the addition of microsilica are somewhat different in comparison with control samples (without additives). Three characteristic areas can also be distinguished here. After 30 cycles of chloride attack, the loss of compressive strength is insignificant for all types of concrete and amounts to 2.7% for V concrete, 1.2% for C concrete, and 0.7% for VC concrete. After 60 inclusive cycles, the trend of change in the rate of loss of compressive strength already has a sharper decreasing character. The loss of compressive strength for V concretes was 8.4%, for C concretes 4.7%, and 3.2% for VC concretes. An even more intense decrease in compressive strength begins after 60 cycles and, finally, after 90 cycles of aggressive chloride exposure, the maximum strength loss for V concretes was 17.0%, for C concretes 11.7%, and 8.6% for VC concretes. In general, the inclusion of a modifying additive has a positive effect, which is expressed in a decrease in the speed of the compressive strength degradation, which undoubtedly increases the resistance of concrete to cyclic chloride attack of the “dry-wet” type.

Figure 9 shows the dependence of the change in compressive strength of concrete samples with an additive in the amount of 4% by weight of the binder on the number of cycles of chloride attack.

Dependences of the strength presented in Figure 9 at 4% microsilica on the number of cycles of chloride attack are well described by Equations (7)–(9) by polynomials of the second degree.

$$R_{b,cub}^V = 43.21 - 0.01563 x - 0.0005757 x^2, \quad R^2 = 0.963 \quad (7)$$

$$R_{b,cub}^C = 45.606 - 0.00356 x - 0.0005568 x^2, \quad R^2 = 0.974 \quad (8)$$

$$R_{b,cub}^{VC} = 47.568 + 0.01516 x - 0.0003143 x^2, \quad R^2 = 0.950 \quad (9)$$

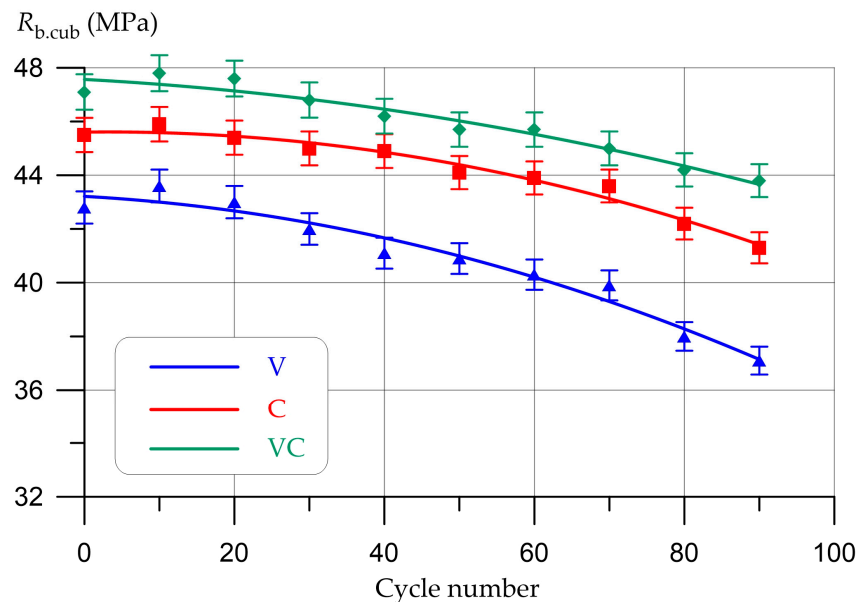


Figure 9. Change in compressive strength of samples V, C, and VC of concrete with 4% silica fume depending on the number of cycles of chloride attack.

Analyzing the compressive strength change curves in Figure 9, it can be noted that concretes with 4% microsilica content have a lower rate of strength decline compared to concretes with 2% additive content. So, for example, after 30 cycles of aggressive chloride exposure, the strength loss for V concretes was 1.9%, for C concretes 1.1%, and 0.6% for VC concretes. Additionally, after 60 and 90 cycles, the loss of compressive strength for V concretes was 5.8% and 13.3%; for C concretes, 3.5% and 9.2%; and for VC concretes, 3.0% and 7.0%, respectively. This can be explained by a more optimal dosage of the additive used for the studied concretes, which contributes to the densest homogeneous concrete structure and maximum strength in comparison with other dosages of the additive.

Figure 10 shows the dependence of the change in compressive strength of concrete samples with an additive of 6% by weight of the binder on the number of cycles of chloride attack.

Dependences of the strength presented in Figure 10 at 6% microsilica on the number of cycles of a chloride attack are well-described by Equations (10)–(12) by polynomials of the second degree.

$$R_{b,cub}^V = 41.94 - 0.02893 x - 0.0006515 x^2, \quad R^2 = 0.971 \quad (10)$$

$$R_{b,cub}^C = 44.150 + 0.0004696 x - 0.0006287 x^2, \quad R^2 = 0.964 \quad (11)$$

$$R_{b,cub}^{VC} = 46.349 - 0.01739 x - 0.0003636 x^2, \quad R^2 = 0.958 \quad (12)$$

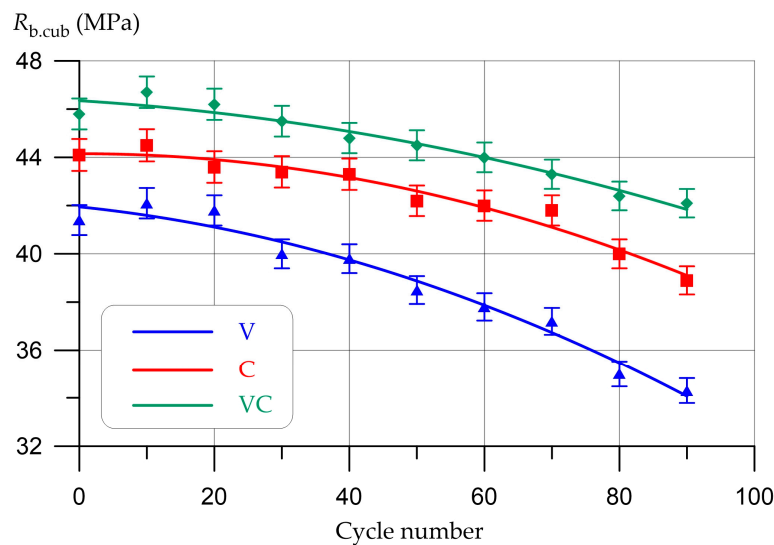


Figure 10. Change in compressive strength of samples V, C, and VC of concrete with 6% silica fume depending on the number of cycles of chloride attack.

The nature of the compressive strength curves of concrete with 6% modifying additive already has a sharper drop in comparison with the strength curves of concrete with 4% content of this additive. That is, starting from 6%, the effectiveness of the influence of the introduction of a modifying additive on the nature of the change in compressive strength, depending on the number of chloride attack cycles, decreases. After 30 cycles of aggressive action, the loss of strength for V concretes was 3.4%, for C concretes 1.6%, and 1.5% for VC concretes. Additionally, after 60 and 90 cycles, the loss of compressive strength for V concretes was 8.7% and 16.2%; for C concretes, 4.8% and 10.7%; and for VC concretes, 4.4% and 8.1%, respectively.

Figure 11 shows the dependence of the change in compressive strength of concrete samples with an additive of 8% by weight of the binder on the number of cycles of chloride attack.

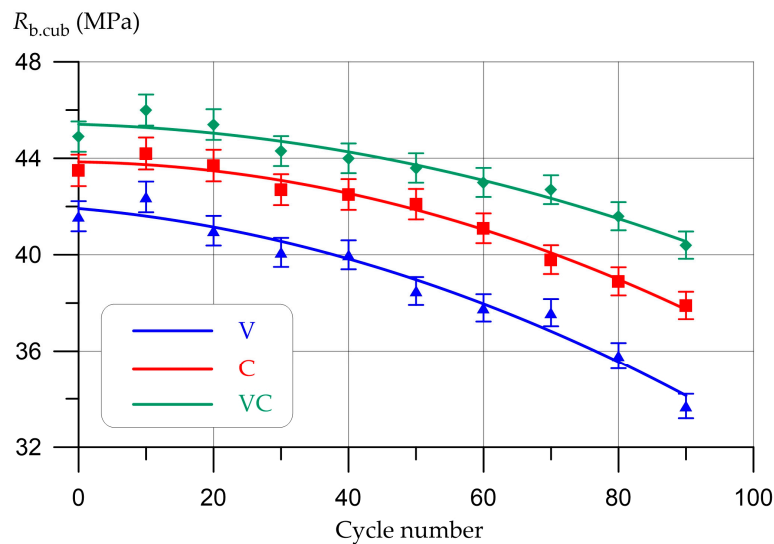


Figure 11. Change in compressive strength of samples V, C, and VC of concrete with 8% silica fume depending on the number of cycles of chloride attack.

Dependences of the strength presented in Figure 11 at 8% microsilica on the number of cycles of chloride attack are well described by Equations (13)–(15) by polynomials of the second degree.

$$R_{b.cub}^V = 41.91 - 0.02478 x - 0.0006856 x^2, \quad R^2 = 0.968 \quad (13)$$

$$R_{b.cub}^C = 43.85 - 0.00425 x - 0.0007083 x^2, \quad R^2 = 0.983 \quad (14)$$

$$R_{b.cub}^{VC} = 45.41 - 0.008318 x - 0.0005075 x^2, \quad R^2 = 0.950 \quad (15)$$

Figure 11 shows that with a microsilica content of 8%, the effectiveness of the influence of the introduction of a modifying additive on the nature of the change in compressive strength depending on the number of cycles of chloride attack also continues to decrease.

Thus, after analyzing the obtained results, it can be concluded that the inclusion of a microsilica additive in the amount of 4% instead of a part of the binder for V, C, and VC concretes is the most effective. There is an increase in compressive strength for all the considered types of concrete, and after 90 cycles of chloride attack, V, C, and VC concretes have the lowest percentage of strength loss. Increasing the strength and improving the structure formation of the composite due to a rationally selected amount of microsilica modifying additive allows for improving the resistance to chloride attack and thereby increases the durability of products and structures made of such concretes.

In general, according to the results of experimental studies, of all the considered types of concrete, vibro-centrifuged concretes demonstrated the highest resistance to chloride attack. For a clearer interpretation and understanding of the effect of concrete manufacturing technology and microsilica modifying additives on the resistance of concrete to dry-wet chloride attack, the following comparative diagrams were constructed (Figure 12).

Based on the results of experimental studies, it was found that vibro-centrifuged concrete has the most effective resistance to chlorides in comparison with centrifuged and especially vibrated concrete. Loss of strength in VC concrete after 90 cycles of chloride attack is 87% less than in V concrete and 24% less compared to C concrete. When using the modifying additive microsilica of the optimal amount, equal to 4% instead of a part of the binder, the strength loss of concrete of various technologies is reduced from 45% to 55% in comparison with compositions without additives. The total loss of strength of vibro-centrifuged concrete with 4% microsilica decreased by 188%, that is, almost two times, in comparison with vibrated concrete without a modifying additive. Thus, the complex recipe-technological effect obtained in this study from the use of vibro-centrifugation technology and a rationally selected amount of a modifying additive in the form of microsilica made it possible to reduce the rate of decline in the strength characteristics of concrete by almost two times, which made it possible to increase the durability of concrete and, accordingly, products and structures from it when exposed to chlorides.

3.3. Study of the Microstructure of Various Types of Concrete Modified with Silica Fume

Figures 13–15 show photographs of the microstructure of samples taken from vibrated, centrifuged, and vibro-centrifuged concretes modified with 4% microsilica after 90 cycles of chloride attack.

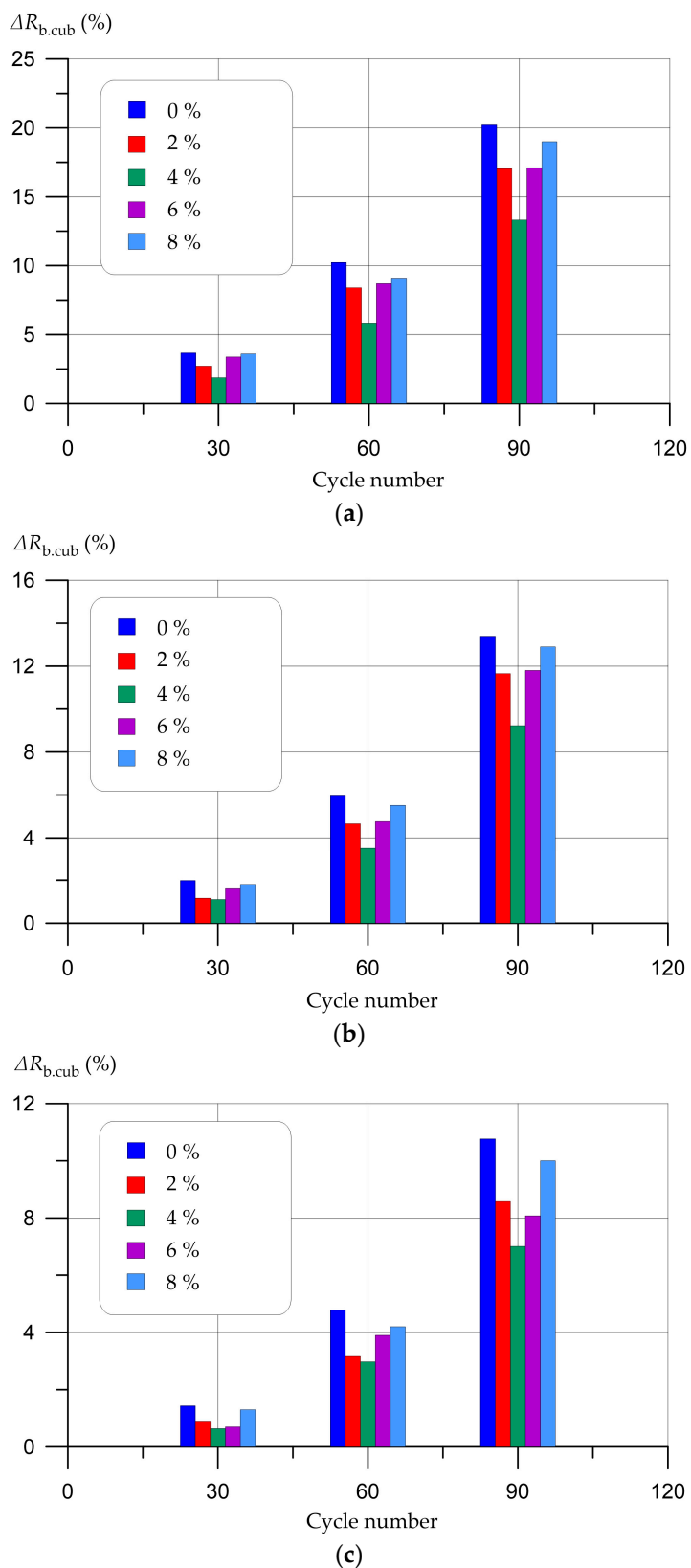


Figure 12. Change in compressive strength of concrete subjected to cyclic chloride action depending on the number of cycles of chloride attack and the content of the modifying additive: (a) V; (b) C; (c) VC.

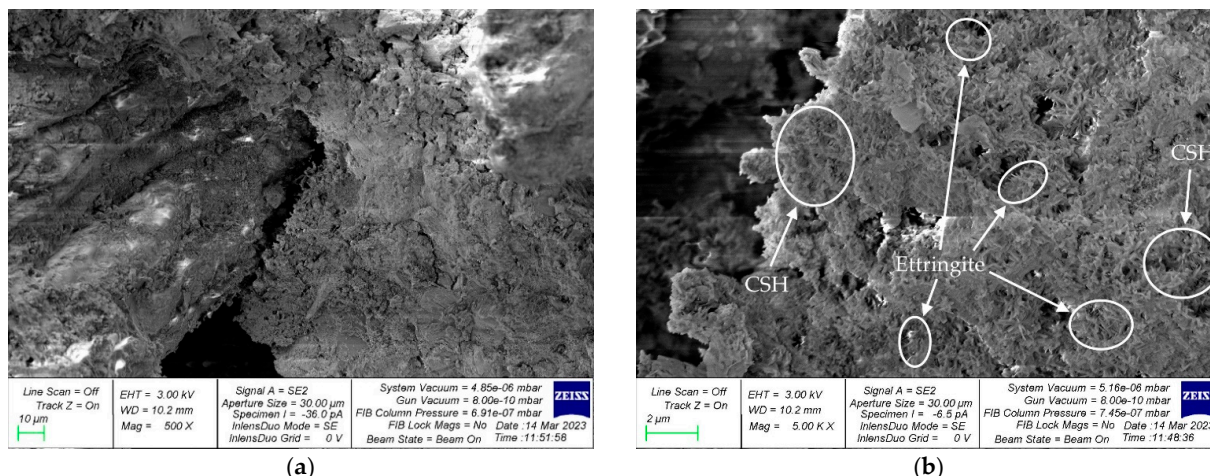


Figure 13. Photographs of the microstructure of a sample taken from vibrated concrete with 4% silica fume: (a) 500 \times ; (b) 5000 \times .

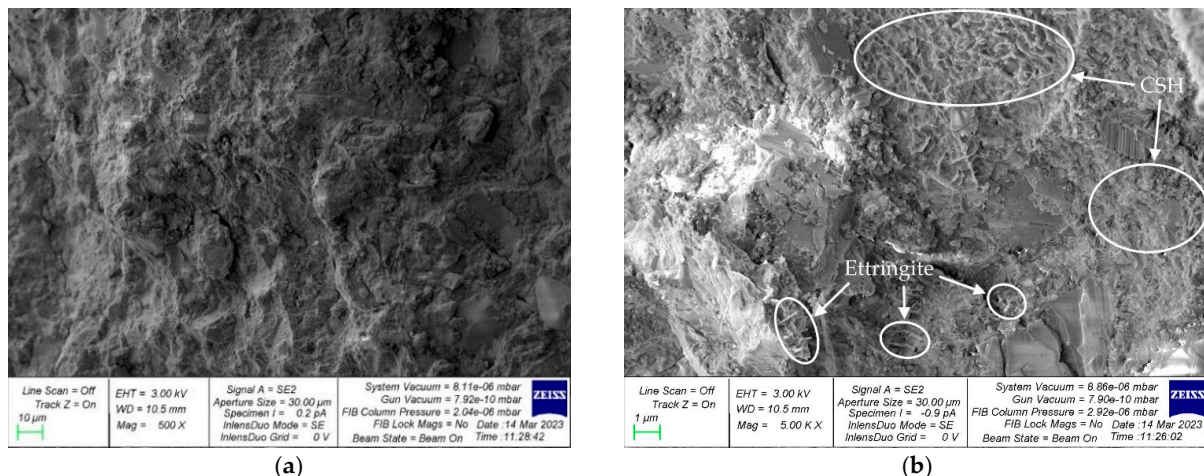


Figure 14. Photographs of the microstructure of a sample taken from centrifuged concrete with 4% silica fume: (a) 500 \times ; (b) 5000 \times .

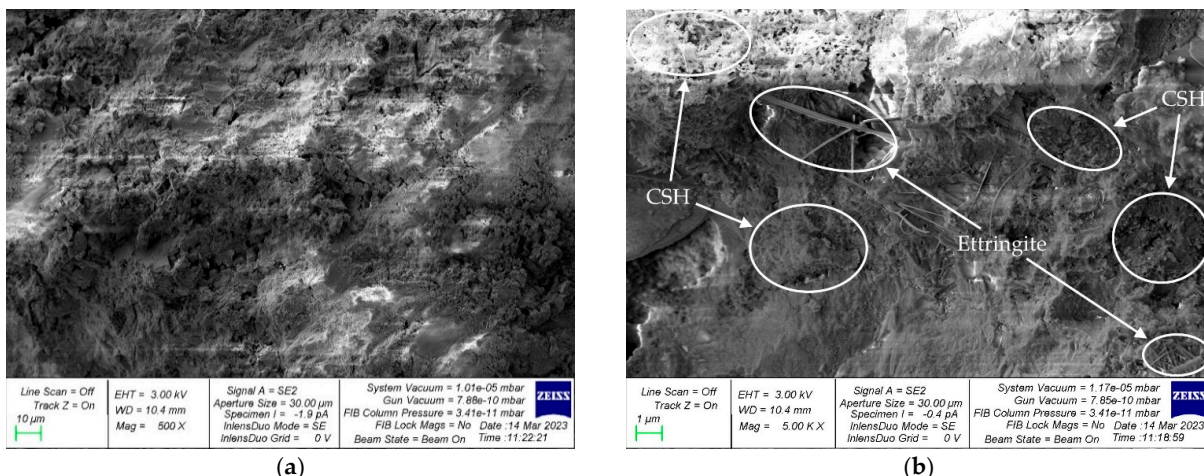


Figure 15. Photographs of the microstructure of a sample taken from vibro-centrifuged concrete with 4% silica fume: (a) 500 \times ; (b) 5000 \times .

Modification of concrete with microsilica provides a denser matrix microstructure and also promotes the formation of additional calcium hydroxilates (CSH), which fill

the contact zones between the binder and the aggregate, thereby compacting the structure and increasing the strength of the concrete (Figures 13b, 14b and 15b). In general, the mechanisms of the effect of microsilica addition on the change in the properties of both conventional vibrated concrete and variotropic concretes, centrifuged and vibro-centrifuged, practically do not differ and are expressed not only in an increase in hydraulic activity but also in the formation of crystallization centers by the smallest particles in the contact zone of cement, additionally increase the strength of hardened cement paste and concrete. The strongest crystallization structures are formed when cement neoplasms are localized on the reaction surfaces of the particles of the mineral additive, and structurally similar hydrosilicates are formed in the contact zone. Microsilica addition is both a substrate for the crystallization of neoplasms and an additional source of structurally active CSH [50,51]. Based on the photographs above, it can be seen that centrifuged (Figure 14a) and vibro-centrifuged (Figure 15a) concretes have a denser structure than vibrated concretes (Figure 13a). Additionally, in variotropic concrete, there is more accumulation of CSH zones (Figures 14b and 15b) than in conventional vibrated concrete (Figure 13b). As for the areas of accumulation of ettringite crystals, centrifuged (Figure 14b) and vibro-centrifuged (Figure 15b) have fewer crystals than vibrated concretes (Figure 13b).

The results obtained in the course of experimental and theoretical studies need to be analyzed because they need to be compared with the results obtained earlier by other authors. Once again, we emphasize the exceptional scientific novelty of our study, which consists of the fact that for the first time, the resistance to chloride corrosion of concrete of the so-called variotropic structure, modified by the addition of microsilica, was studied. That is, the previously studied, as well as the vibrated concretes obtained by us under conditions of chloride attack with variotropic concretes modified with microsilica, were compared with each other in the course of our experimental studies. The simulated chloride attack conditions for concretes of various technologies of vibrating, centrifuging, and vibro-centrifuging, in comparison with the results of other authors, gave interesting results and set the ground for reflection and formed the prospects for future research on this topic. Explaining the obtained results, it should be emphasized that, as it was supposed in the working hypothesis, the variotropic vibro-centrifuged concrete showed the greatest resistance to chloride attack, which can be explained by its special structure and nature, and the mechanism of its formation. As is known earlier from our works [5,45,46,49,52–54], as well as from the works of other authors [55–57], during centrifugal compaction of both centrifuged and vibro-centrifuged concretes, a variotropic structure is formed, which includes conditional three layers: outer, middle, and inner. At the same time, the specifics of the transport infrastructure structures being erected presupposes a closed configuration of such reinforced concrete structures that contribute to maximum protection against the penetration of chloride attack subjects into the body of the structure. This is due to the denser structure of the outer layer with the closed nature of microporosity, which is somehow present in a conditional form in the outer layer, the most effective control of the structure formation of such structures at the stage of their manufacture. We emphasize that the centrifuged sample also showed fairly high resistance to a chloride attack. But in view of the fact that the vibro-centrifuged sample has an improved variotropic structure with closed micro and macroporosity in the outer layer, and this structure can be controlled by prescription and technological factors at the manufacturing stage, all this contributes to the creation of the most promising and advanced variotropic reinforced concrete vibro-centrifuged structures intended for transport facilities infrastructure.

The results obtained in this study are also in good agreement with a number of other studies where the addition of microsilica was used to increase the resistance of cement composites to various types of aggressive impact. For example, in [13], the introduction of a nanosilica additive into the composition of a cement slurry makes it possible to significantly reduce the diffusion coefficient of chloride ions. In a study [58], replacing part of the cement with 10% microsilica allows concrete with the best corrosion properties to be obtained. Additionally, the positive effect of the addition of microsilica on the characteristics of

concretes operated in various environments with the presence of chloride exposure is confirmed by the results of studies [59–61].

It has been established that in variotropic concretes, the effect of the introduction of microsilica on increasing resistance to chloride attack is not inferior to the effect of the introduction of microsilica in conventional concrete and varies from 45% to 55% depending on the type of technology for producing a composite. Thus, a complex recipe-technological effect of increasing the resistance to chloride attack of concrete by creating a variotropic structure (technological factor) and by using a modifying additive of microsilica (recipe factor), exceeding the effect of the use of microsilica in conventional vibrated concrete, has been proved. The complex effect, expressed as a decrease in strength loss as a result of cyclic chloride attack, amounted to 188%.

4. Conclusions

Based on the results of experimental studies of the resistance of vibrated, centrifuged, and vibro-centrifuged concrete to cyclic chloride attack, the following conclusions were formulated:

- (1) Vibro-centrifuged concretes have the highest resistance to cyclic aggressive chloride attack, which is primarily expressed by a lower percentage drop in compressive strength compared to vibrated (by 87%) and centrifuged concretes (by 24%);
- (2) The use of a microsilica modifying agent in the amount of 2–6% instead of part of the binder has a positive effect on the resistance of concrete to cyclic chloride attack. The most effective is the introduction of additives in the amount of 4%. Reducing the loss of strength of vibrated, centrifuged, and vibro-centrifuged concrete after 90 “dry-wet” cycles as a result of the use of a modifier of a rationally selected amount ranged from 45% to 55%, depending on the type of technology for producing a composite. In variotropic concretes, the effect of introducing microsilica on increasing resistance to chloride attack is not inferior to the effect of introducing microsilica in conventional concrete;
- (3) A complex recipe-technological effect of increasing the resistance to chloride attack of concrete by creating a variotropic structure (technological factor) and by using a modifying additive of microsilica (recipe factor), exceeding the effect of the use of microsilica in conventional vibrated concrete, has been proved. The complex effect, expressed as a decrease in strength loss as a result of cyclic chloride attack, amounted to 188%, that is, almost two times;
- (4) The structure of the composite, as a result of a complex formulation and technological solution, has become denser and stronger due to the formation of a larger amount of cement gel. As a result, the strength and durability of concrete increased under cyclic chloride exposure.

The practical significance of the study is the proven increased ability of variotropic concretes to resist chloride attack, which makes it possible to foresee these results in the practice of designing and building infrastructure facilities.

Prospects for the development of research lie in the direction of research on full-scale reinforced concrete structures under conditions of chloride attack. A promising direction is the modeling of such infrastructure facilities, taking into account the obtained data on concrete and comparing the modeling results with experimental data. Potential operating limitations may be caused by some differences in the plant's technological capacities for the production of centrifuged and vibro-centrifuged concrete and the pilot laboratory plant. That is why the main task at the next stage of the study will be the pilot testing of the results obtained on large-scale full-size reinforced concrete centrifuged and vibro-centrifuged structures.

Author Contributions: Conceptualization, S.A.S., E.M.S., A.N.B. and D.E.; methodology, S.A.S., E.M.S. and A.C.; software, O.A., S.A.S., E.M.S., A.N.B. and A.C.; validation, D.E., S.A.S., E.M.S. and A.N.B.; formal analysis, A.C., S.A.S. and E.M.S.; investigation, O.A., D.E., L.R.M., S.A.S., E.M.S., A.N.B. and B.M.; resources, B.M. and V.V.; data curation, S.A.S., E.M.S. and A.C.; writing—original draft preparation, S.A.S., E.M.S. and A.N.B.; writing—review and editing, S.A.S., E.M.S. and A.N.B.; visualization, V.V., S.A.S., E.M.S. and A.N.B.; supervision, L.R.M. and B.M.; project administration, L.R.M. and B.M.; funding acquisition, A.N.B. and B.M. All authors have read and agreed to the published version of the manuscript.

Funding: This research received no external funding.

Data Availability Statement: The study did not report any data.

Acknowledgments: The authors would like to acknowledge the administration of Don State Technical University for their resources and financial support.

Conflicts of Interest: The authors declare no conflict of interest.

References

- Burdumos-Nergis, D.D. Special Issue “Advanced Engineering Cementitious Composites and Concrete Sustainability”. *Materials* **2023**, *16*, 2582. [CrossRef] [PubMed]
- Poursaei, A.; Ross, B. The Role of Cracks in Chloride-Induced Corrosion of Carbon Steel in Concrete—Review. *Corros. Mater. Degrad.* **2022**, *3*, 258–269. [CrossRef]
- Gopu, G.; Joseph, S. Corrosion Behavior of Fiber-Reinforced Concrete—A Review. *Fibers* **2022**, *10*, 38. [CrossRef]
- Ukpata, J.; Ogirigbo, O.; Black, L. Resistance of Concretes to External Chlorides in the Presence and Absence of Sulphates: A Review. *Appl. Sci.* **2023**, *13*, 182. [CrossRef]
- Shcherban’, E.M.; Stel’makh, S.A.; Beskopylny, A.N.; Mailyan, L.R.; Meskhi, B.; Elshaeva, D.; Chernil’nik, A. Physical and Mechanical Characteristics of Variotropic Concrete during Cyclic and Continuous Sulfate Attack. *Appl. Sci.* **2023**, *13*, 4386. [CrossRef]
- Wang, C. Explicitly Assessing the Durability of RC Structures Considering Spatial Variability and Correlation. *Infrastructures* **2021**, *6*, 156. [CrossRef]
- Su, D.; Pang, J.; Huang, X. Experimental Study on the Influence of Rubber Content on Chloride Salt Corrosion Resistance Performance of Concrete. *Materials* **2021**, *14*, 4706. [CrossRef]
- Zhu, R.; Pang, J.; Wang, T.; Huang, X. Experimental Research on Chloride Erosion Resistance of Rubber Concrete. *Adv. Civ. Eng.* **2020**, *2020*, 3972405. [CrossRef]
- Elsayed, M.; Tayeh, B.; Taha, Y.; El-Azim, A. Experimental investigation on the behaviour of crumb rubber concrete columns exposed to chloride–sulphate attack. *Structures* **2022**, *46*, 246–264. [CrossRef]
- Zhang, Y.; Cui, M.; Chen, G.; Han, W. Experimental study of the effects of graphene nanoplatelets on microstructure and compressive properties of concrete under chloride ion corrosion. *Constr. Build. Mater.* **2022**, *360*, 129564. [CrossRef]
- Qi, X.; Zhang, S.; Wang, T.; Guo, S.; Ren, R. Effect of High-Dispersible Graphene on the Strength and Durability of Cement Mortars. *Materials* **2021**, *14*, 915. [CrossRef]
- Chousidis, N.; Zacharopoulou, A.; Batis, G.; Zeris, C. Effect of Carbon Nanotubes (CNTs) on Chloride Penetration Resistance and Physical-Mechanical Properties of Cementitious Materials. *Mater. Proc.* **2021**, *6*, 9934. [CrossRef]
- Liu, X.; Liu, R.; Xie, X.; Zuo, J.; Lyu, K.; Shah, S. Chloride corrosion resistance of cement mortar with recycled concrete powder modified by nano-silica. *Constr. Build. Mater.* **2023**, *364*, 129907. [CrossRef]
- Liang, X.; Qi, W.; Fang, Z.; Zhang, S.; Fan, Y.; Shah, S. Study on the Relationship between Chloride Ion Penetration and Resistivity of NAC-Cement Concrete. *Buildings* **2022**, *12*, 2044. [CrossRef]
- Hassan, M.; Elahi, A.; Asad, M. Performance of Fibre Reinforced Self Compacting Concrete against Chloride Attack. *Eng. Proc.* **2022**, *22*, 5. [CrossRef]
- Afroughsabet, V.; Biolzi, L.; Monteiro, P. The effect of steel and polypropylene fibers on the chloride diffusivity and drying shrinkage of high-strength concrete. *Compos. B Eng.* **2018**, *139*, 84–96. [CrossRef]
- Luo, Y.; Niu, D.; Su, L. Chloride Diffusion Property of Hybrid Basalt–Polypropylene Fibre-Reinforced Concrete in a Chloride–Sulphate Composite Environment under Drying–Wetting Cycles. *Materials* **2021**, *14*, 1138. [CrossRef]
- Ghorbani, S.; Taji, I.; Tavakkolizadeh, M.; Davodi, A.; Brito, J. Improving corrosion resistance of steel rebars in concrete with marble and granite waste dust as partial cement replacement. *Constr. Build. Mater.* **2018**, *185*, 110–119. [CrossRef]
- Sullivan, M.S.; Chorzepa, M.G.; Durham, S.A. Characterizing the Performance of Ternary Concrete Mixtures Involving Slag and Metakaolin. *Infrastructures* **2020**, *5*, 14. [CrossRef]
- Subpa-as, P.; Nito, N.; Fujiwara, S.; Date, S. Evaluation of the Prediction and Durability on the Chloride Penetration in Cementitious Materials with Blast Furnace Slag as Cement Addition. *Constr. Mater.* **2022**, *2*, 5. [CrossRef]
- Zhong, X.; Li, J.; Xu, J.; Wang, K.; Zhu, B.; Liu, Y.; Ni, K. Deterioration of Mechanical Properties of Axial Compression Concrete Columns with Corroded Stirrups Coupling on Load and Chloride. *Appl. Sci.* **2023**, *13*, 2423. [CrossRef]

22. Lee, K.-M.; Yoon, Y.-S.; Yang, K.-H.; Yoo, B.-Y.; Kwon, S.-J. Corrosion Behavior in RC Member with Different Cover Depths under Cyclic Chloride Ingress Conditions for 2 Years. *Appl. Sci.* **2022**, *12*, 13002. [[CrossRef](#)]
23. Cui, F.; Song, L.; Wang, X.; Li, M.; Hu, P.; Deng, S.; Zhang, X.; Li, H. Seismic Fragility Analysis of the Aging RC Columns under the Combined Action of Freeze–Thaw Cycles and Chloride-Induced Corrosion. *Buildings* **2022**, *12*, 2223. [[CrossRef](#)]
24. Chen, G.; Wang, M.; Cui, C.; Zhang, Q. Corrosion-Fatigue Life Prediction of the U-Shaped Beam in Urban Rail Transit under a Chloride Attack Environment. *Materials* **2022**, *15*, 5902. [[CrossRef](#)] [[PubMed](#)]
25. Chen, W.; Liu, Y.; Qian, H.; Wu, P.; Wu, Y.; Liu, F. Chloride Ion Corrosion Resistance of Innovative Self-Healing SMA Fiber-Reinforced Engineering Cementitious Composites under Dry-Wet Cycles for Ocean Structures. *Buildings* **2023**, *13*, 518. [[CrossRef](#)]
26. Kumar, M.; Mini, K.; Rangarajan, M. Ultrafine GGBS and calcium nitrate as concrete admixtures for improved mechanical properties and corrosion resistance. *Constr. Build. Mater.* **2018**, *182*, 249–257. [[CrossRef](#)]
27. Dheyaaldin, M.; Mosaberpanah, M.; Alzeebaree, R. The Effect of Nano-Silica and Nano-Alumina with Polypropylene Fiber on the Chemical Resistance of Alkali-Activated Mortar. *Sustainability* **2022**, *14*, 16688. [[CrossRef](#)]
28. Yu, Y.; Wang, J.; Wang, N.; Wu, C.; Zhang, X.; Wang, D.; Ma, Z. Combined Freeze–Thaw and Chloride Attack Resistance of Concrete Made with Recycled Brick-Concrete Aggregate. *Materials* **2021**, *14*, 7267. [[CrossRef](#)]
29. Arreola-Sanchez, M.; Alonso-Guzman, E.; Martinez-Molina, W.; Torres-Acosta, A.; Chavez-Garcia, H.; Ponce-Ortega, J. Reinforced Concrete Structure Performance in Marine Structures: Analyzing Durability Indexes to Obtain More Accurate Corrosion Initiation Time Predictions. *Materials* **2021**, *14*, 7662. [[CrossRef](#)]
30. Valencia-Saavedra, W.; Aguirre-Guerrero, A.; Gutiérrez, R. Assessment of the Corrosion of Steel Embedded in an Alkali-Activated Hybrid Concrete Exposed to Chlorides. *Molecules* **2022**, *27*, 5296. [[CrossRef](#)]
31. Farzad, M.; Fancy, S.F.; Lau, K.; Azizinamini, A. Chloride Penetration at Cold Joints of Structural Members with Dissimilar Concrete Incorporating UHPC. *Infrastructures* **2019**, *4*, 18. [[CrossRef](#)]
32. Lee, J.-M.; Hong, S.; Yang, H.; Jung, D.-H. Numerical Modeling of Chloride Transport in Concrete under Cyclic Exposure to Chloride. *Materials* **2022**, *15*, 5966. [[CrossRef](#)]
33. Zacchei, E.; Nogueira, C. Numerical Solutions for Chloride Diffusion Fluctuation in RC Elements from Corrosion Probability Assessments. *Buildings* **2022**, *12*, 1211. [[CrossRef](#)]
34. Zacchei, E.; Bastidas-Arteaga, E. Multifactorial Chloride Ingress Model for Reinforced Concrete Structures Subjected to Unsaturated Conditions. *Buildings* **2022**, *12*, 107. [[CrossRef](#)]
35. El Hajj, B.; Castanier, B.; Schoefs, F.; Bastidas-Arteaga, E. Stochastic Multiphasic Multivariate State-Based Degradation and Maintenance Meta-Models for RC Structures Subject to Chloride Ingress. *Infrastructures* **2023**, *8*, 36. [[CrossRef](#)]
36. Robles, K.; Yee, J.-J.; Kee, S.-H. Electrical Resistivity Measurements for Nondestructive Evaluation of Chloride-Induced Deterioration of Reinforced Concrete—A Review. *Materials* **2022**, *15*, 2725. [[CrossRef](#)]
37. Sun, C.; Sun, M.; Liu, J.; Dong, Z.; Fan, L.; Duan, J. Anti-Corrosion Performance of Migratory Corrosion Inhibitors on Reinforced Concrete Exposed to Varying Degrees of Chloride Erosion. *Materials* **2022**, *15*, 5138. [[CrossRef](#)]
38. Malan, J.D.; van Rooyen, A.S.; van Zijl, G.P.A.G. Chloride Induced Corrosion and Carbonation in 3D Printed Concrete. *Infrastructures* **2022**, *7*, 1. [[CrossRef](#)]
39. GOST R 58894-2020 Silica Fume for Concretes and Mortars. Specifications. Available online: <https://docs.cntd.ru/document/1200173805> (accessed on 1 May 2023).
40. GOST R 57345-2016/EN 206-1:2013 Concrete. General Specifications. Available online: <https://docs.cntd.ru/document/1200142845> (accessed on 1 May 2023).
41. VSN 1-90 Fabrication Requirements for Centrifugal-Cast Support Pillars for Contact Lines, Communications Lines, and Lock-Out Systems. Available online: <https://meganorm.ru/Index2/1/4294851/4294851029.htm> (accessed on 1 May 2023).
42. GOST R 57813-2017/EN 12350-6:2009 Testing Fresh Concrete—Part 6. Density. Available online: <https://docs.cntd.ru/document/1200157335> (accessed on 1 May 2023).
43. GOST R 57809-2017/EN 12350-2:2009 Testing Fresh Concrete—Part 2. Slump Test. Available online: <https://docs.cntd.ru/document/1200157288> (accessed on 1 May 2023).
44. Stel'makh, S.A.; Shcherban', E.M.; Kholodnyak, M.G.; Nasevich, A.S.; Yanovskaya, A.V. Device for the Manufacture of Products from Vibrocentrifuged Concrete. Russian. Federation Patent 197,610, 29 January 2020. Available online: <https://patentimages.storage.googleapis.com/99/a7/e4/7331df00d4bdb/RU197610U1.pdf> (accessed on 1 May 2023).
45. Beskopylny, A.N.; Shcherban, E.M.; Stel'makh, S.A.; Mailyan, L.R.; Meskhi, B.; Chernil'nik, A.; El'shaeva, D. Influence of Variotropy on the Evaluation of Strength Properties and Structure Formation of Concrete under Freeze–Thaw Cycles. *J. Compos. Sci.* **2023**, *7*, 58. [[CrossRef](#)]
46. Beskopylny, A.N.; Stel'makh, S.A.; Shcherban', E.M.; Mailyan, L.R.; Meskhi, B.; Chernil'nik, A.; El'shaeva, D.; Pogrebnyak, A. Influence of Variotropy on the Change in Concrete Strength under the Impact of Wet–Dry Cycles. *Appl. Sci.* **2023**, *13*, 1745. [[CrossRef](#)]
47. GOST 10180 Concretes. Methods for Strength Determination Using Reference Specimens. Available online: <http://docs.cntd.ru/document/1200100908> (accessed on 1 May 2023).

48. Moskvin, V.M.; Ivanov, F.M.; Alekseev, S.N.; Guzeev, E.A. *Corrosion of Concrete and Reinforced Concrete, Methods of Their Protection*; Stroyizdat: Moscow, Russia, 1980; 536p. Available online: <https://search.rsl.ru/ru/record/01001015979> (accessed on 2 May 2023).
49. Beskopylny, A.N.; Stel'makh, S.A.; Shcherban', E.M.; Mailyan, L.R.; Meskhi, B.; Beskopylny, N.; El'shaeva, D.; Kotenko, M. The Investigation of Compacting Cement Systems for Studying the Fundamental Process of Cement Gel Formation. *Gels* **2022**, *8*, 530. [CrossRef] [PubMed]
50. Zaychenko, N.M.; Ali, S.A.S.K.; Sakhoshko, E.V. Influence of organic mineral modifier on the base of condensed microsilica and (PNS+PCE) superplasticizers on the properties and of cement paste stone microstructure. *Mod. Ind. Civ. Constr.* **2009**, *5*, 187–195.
51. Olginskii, A.G. Peculiarities of Contact Formation in Cement Concrete with Mineral Microfiller. *Proc. DonNACEA* **2004**, *1*, 134–140.
52. Beskopylny, A.N.; Meskhi, B.; Stel'makh, S.A.; Shcherban', E.M.; Mailyan, L.R.; Veremeenko, A.; Akopyan, V.; Shilov, A.V.; Chernil'nik, A.; Beskopylny, N. Numerical Simulation of the Bearing Capacity of Variotropic Short Concrete Beams Reinforced with Polymer Composite Reinforcing Bars. *Polymers* **2022**, *14*, 3051. [CrossRef] [PubMed]
53. Beskopylny, A.N.; Shcherban', E.M.; Stel'makh, S.A.; Mailyan, L.R.; Meskhi, B.; Evtushenko, A.; Varavka, V.; Beskopylny, N. Nano-Modified Vibrocentrifuged Concrete with Granulated Blast Slag: The Relationship between Mechanical Properties and Micro-Structural Analysis. *Materials* **2022**, *15*, 4254. [CrossRef]
54. Beskopylny, A.; Stel'makh, S.A.; Shcherban', E.M.; Mailyan, L.R.; Meskhi, B. Nano modifying additive micro silica influence on integral and differential characteristics of vibrocentrifuged concrete. *J. Build. Eng.* **2022**, *51*, 104235. [CrossRef]
55. Akhverdov, I.N. *Reinforced Concrete Pressure Centrifuged Pipes*; Stroyizdat: Moscow, Russia, 1967; 164p, Available online: <https://search.rsl.ru/ru/record/01005953134> (accessed on 2 May 2023).
56. Kliukas, R.; Lukoševičienė, O.; Jaras, A.; Jonaitis, B. The Mechanical Properties of Centrifuged Concrete in Reinforced Concrete Structures. *Appl. Sci.* **2020**, *10*, 3570. [CrossRef]
57. Feng, B.; Zhu, Y.-H.; Xie, F.; Chen, J.; Liu, C.-B. Experimental Investigation and Design of Hollow Section, Centrifugal Concrete-Filled GFRP Tube Columns. *Buildings* **2021**, *11*, 598. [CrossRef]
58. Ghanei, A.; Eskandari-Naddaf, H.; Ozbakkaloglu, T.; Davoodi, A. Electrochemical and statistical analyses of the combined effect of air-entraining admixture and micro-silica on corrosion of reinforced concrete. *Constr. Build. Mater.* **2020**, *262*, 120768. [CrossRef]
59. Valipour, M.; Pargar, F.; Shekarchi, M.; Khani, S.; Moradian, M. In situ study of chloride ingress in concretes containing natural zeolite, metakaolin and silica fume exposed to various exposure conditions in a harsh marine environment. *Constr. Build. Mater.* **2013**, *46*, 63–70. [CrossRef]
60. Ahmad, S.; Al-Amoudi, O.S.B.; Khan, S.M.S.; Maslehuddin, M. Effect of silica fume inclusion on the strength, shrinkage and durability characteristics of natural pozzolan-based cement concrete. *Case Stud. Constr. Mater.* **2022**, *17*, e01255. [CrossRef]
61. Fu, Q.; Zhang, Z.; Wang, Z.; He, J.; Niu, D. Erosion behavior of ions in lining concrete incorporating fly ash and silica fume under the combined action of load and flowing groundwater containing composite salt. *Case Stud. Constr. Mater.* **2022**, *17*, e01659. [CrossRef]

Disclaimer/Publisher's Note: The statements, opinions and data contained in all publications are solely those of the individual author(s) and contributor(s) and not of MDPI and/or the editor(s). MDPI and/or the editor(s) disclaim responsibility for any injury to people or property resulting from any ideas, methods, instructions or products referred to in the content.